tension of our work.

This work was done at Tohoku University while one of us (J.J.R.) stayed in Japan. The kind hospitality and support of Tohoku University are gratefully acknowledged. We thank Professor T. Sato and Professor K. Nishihara for helpful discussions.

[1]P. Carlqvist, in *Wave Instabilities in Space Plasmas*, edited by P. J. Palmadesso and K. Papadopoulos (Reidel, Dordrecht, 1979), p. 83; S. Torvén, *ibid.*, p. 109. See also works referred to in the above papers.

[2]I. B. Bernstein *et al.*, Phys. Rev. 108, 546 (1957); G. Knorr and C. K. Goertz, Astrophys. Space Sci. 31, 209 (1974).

[3]J. S. DeGroot *et al.*, Phys. Rev. Lett. 38, 1283 (1977); T. Sato and H. Okuda, Phys. Rev. Lett. 44, 740 (1980).

[4]H. Alfvén and P. Carlqvist, Sol. Phys. 1, 220 (1967).

[5]F. S. Mozer *et al.*, Phys. Rev. Lett. 38, 292 (1977).

[6]P. Coakley and N. Hershkowitz, Phys. Fluids 22, 1171 (1979).

[7]P. Leung *et al.*, Phys. Fluids 23, 992 (1980).

[8]S. Iizuka *et al.*, Phys. Rev. Lett. 43, 1404 (1979).

[9]K. D. Baker *et al.*, in *Proceedings of the International Conference on Plasma Physics* (Fusion Research Association of Japan, Nagoya, 1980), Vol. I, p. 417.

[10]P. Coakley *et al.*, Phys. Lett. 70A, 425 (1979).

[11]S. Torvén and D. Anderson, J. Phys. D 12, 717 (1979).

[12]C. K. Goertz and G. Joyce, Astrophys. Space Sci. 32, 165 (1975); G. Joyce and R. F. Hubbard, J. Plasma Phys. 20, 39 (1978); N. Singh, Plasma Phys. 22, 1 (1980).

[13]R. W. Motley, *Q Machines* (Academic, New York, 1975); N. Sato *et al.*, Phys. Rev. Lett. 34, 931 (1975).

[14]I. Langmuir, Phys. Rev. 33, 954 (1929); L. P. Block, Cosmic Electrodyn. 3, 349 (1972).

[15]D. Bohm, in *The Characteristics of Electrical Discharge in Magnetic Fields*, edited by A. Guthrie and R. K. Wakering (McGraw-Hill, New York, 1949), p. 77.

[16]Recently, S. Iizuka *et al.* (to be published) clarified the dynamics of the broad negative potential dip observed on the low-potential tail of the DL.

[17]R. F. Ellis and R. W. Motley, Phys. Fluids 17, 582 (1974); G. Benford *et al.*, Phys. Fluids 17, 1001 (1974); M. Yamada and H. W. Hendel, Phys. Fluids 21, 1555 (1978).

[18]S. R. Stenzel *et al.*, Phys. Rev. Lett. 45, 1497 (1980).

Filamentary Collapse in Electron-Beam Plasmas

P. J. Christiansen and V. K. Jain

Plasma and Space Physics Group, University of Sussex, Falmer, Brighton BN1 9QH, England

and

L. Stenflo

Department of Plasma Physics, University of Umeå, S-90187 Umeå, Sweden

(Received 11 December 1980)

Observations of a form of three-dimensional turbulence, which occurs in beam-plasma interactions, are described. Large amplitude, beam driven instabilities in both the oblique electron plasma and electron-cyclotron modes are shown to collapse into thin, magnetic field aligned filaments, and to exhibit a variety of modulation time scales characteristic of both electron and ion modes in the system. On the largest time scales, associated density depletions are observed.

PACS numbers: 52.40.Mj, 52.35.Py

In recent years there has been considerable interest in the nonlinear evolution of large-amplitude electron waves in plasmas and in the processes leading to self modulation and formation of solitary or collapsed wave field structures.[1-11] To date, experiments have been carried out in either magnetic-field–free systems, or in very strongly magnetized plasmas leading to quasi–one-dimensional effects.[1-5]

As with some other experiments, in those described here, large-amplitude waves resulting from a beam-plasma interaction form the high-frequency pump for the system. The beam is unmodulated in order to avoid complications arising from the insertion of wave launching antennae and, significantly, because it is of small radius, the unstable waves are rather oblique ($K_\perp > K_\parallel$) to the axial magnetic field, resulting in a quasitransverse pump wave field.

The characteristics of the apparatus are as follows: A thin (0.75-cm-diam) electron beam (current variable up to 7 mA, energy variable in range 150–250 eV) is injected axially from one end of a 10-cm-diam, 150-cm-long glass vessel immersed in a dc axial magnetic field. The beam-produced argon plasma (typical pressure $\sim 10^{-4}$

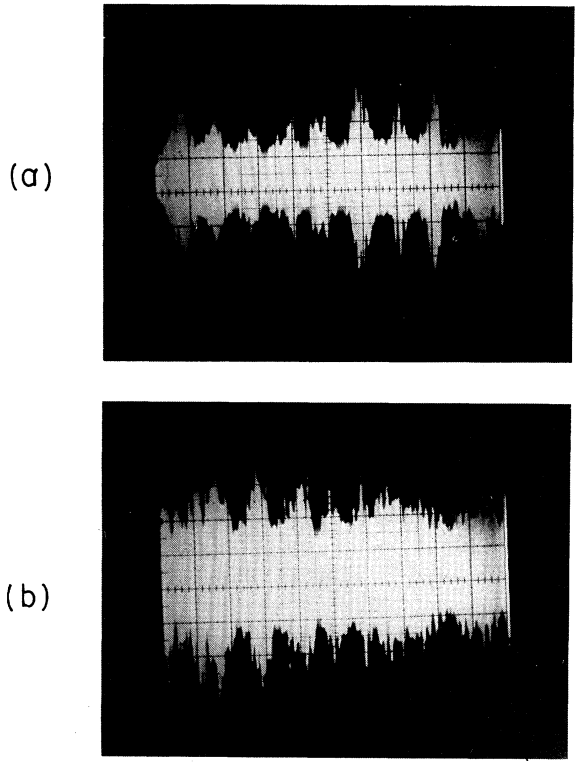

FIG. 1. Real-time observations of wave burst structure. (a) Horizontal scale, 2 μsec/div; vertical scale, 10 mV/div. (b) Horizontal scale, 200 μsec/div; vertical scale, 10 mV/div.

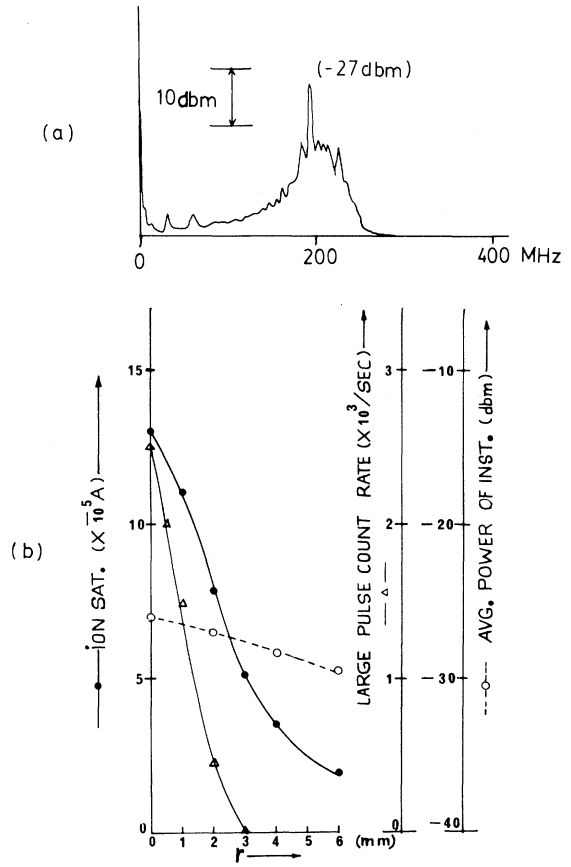

FIG. 2. (a) Frequency spectrum of electron plasma wave. f_{pe} = 300 MHz, f_{ce} = 325 MHz; beam energy = 200 eV; beam current = 3.5 mA. (b) Comparison of radial distribution of large-amplitude pulses ($\geq$ 32 mV peak to peak) with average power of the instability and density profile. Parameters as in (a).

Torr) has a density which is variable in the range 10^8–5×10^9 cm^{-3}, and an electron temperature in the range 2–6 eV. The system is equipped with axially and radially moveable miniature coaxial probes; one of the latter, situated at 66 cm from the gun, has an exposed tip length of 1.5 mm. By varying the parameters of the system, large-amplitude waves in both the electron plasma ($\omega < \omega_{pe}$, ω_{ce}) and the electron cyclotron ($\omega_{uh} \gtrsim \omega > \omega_{ce}$) modes can be excited ($\omega_p/2\pi$ is the plasma frequency; $\omega_{ce}/2\pi$ the electron gyrofrequency; $\omega_{uh}^2 = \omega_{pe}^2 + \omega_{ce}^2$).

In real time, both types of instabilities have a bursty quasirepetitive structure which displays a (nested) hierarchy of time scales, τ, corresponding to those characteristic of low-frequency electron waves ($\tau_1 \sim 1/10 f_{pi}$), ion sound waves ($\tau_2 \sim 10/f_{pi}$, $10/f_{lh}$) and ion cyclotron waves ($\tau_3 \sim 1/f_{ci}$).

Examples of the last two, which are not obvious in conventional spectrum analysis can be seen in Fig. 1, where traces of a large-amplitude oblique electron plasma wave at 200 MHz (recorded on a broadband oscilloscope) are shown on different time scales. Figure 1(b) at the longer time scale shows sets of spiky bursts with a repetitive temporal structure $\tau_3 \sim 200$ μsec compared with $1/f_{ci}$ = 225 μsec. In Fig. 1(a), a sample of an individual spike is shown on shorter time scales, and it too has a spiky and repetitive form $\tau_2 \sim 2$ μsec ($1/f_{pi} \sim 0.9$ μsec).

Note that the oscilloscope storage system used does not capture the full amplitude excursions of the largest individual spikes, which may be a factor of 2–3 greater than shown. Proceeding to even shorter time scales, we find that the individual spikes in Fig. 1(a) are themselves formed by bursts of deeply modulated plasma-wave oscillations with repetition time $\tau_1 \sim 100$ nsec.

In Fig. 2(a) we show the corresponding average

frequency spectrum of these waves. The spectrum is broad and displays features indicative of modulation on the fastest time scale. The most interesting aspect of the large amplitude bursts, i.e., their confinement to the axis of the system, can be seen in Fig. 2(b). In order to record the distribution of these pulses the precalibrated trigger level of the broadband oscilloscope is used as a discriminator, and gate output pulses are fed to a conventional pulse shaping, counting and ratemeter system. The ratemeter output, corresponding to the count rate of pulses above given level is fed continuously to the Y input of a plotter, whose X input registers the radial displacement of the slowly moving radial probe. The radial profile of large pulses thus obtained (identified by open triangles) is compared with the radial density distribution recorded in similar fashion by conventional Langmuir-probe techniques (dots) and also with the average signal profile, detected by a spectrum analyzer set to sweep a range of 40 MHz around the spectral peak of the instability (open circles). The radial scale size, $L \sim 1$ mm, of the pulse distribution, is significantly smaller than that of the density (~3 mm) and average profile (~6 mm). The pulse distribution is centered on the beam axis.

Similar behavior is also found for beam-excited instabilities above f_{ce}, on the upper hybrid branch of the oblique Bernstein mode. In the sample in Fig. 3(a) the power spectrum shows a broad feature centered on 750 MHz ($f_p/f_{ce} \sim 1$) and in Fig. 3(b), the radial distributions of large- and intermediate-amplitude pulses are compared with profiles of the average power and density. Again the largest pulses are centrally confined to regions of radial scale size ~1 mm, corresponding, like those of the plasma mode described above, to a few thermal-electron Larmor radii. By comparison, the larger scale size (~3 mm) of the intermediate-level pulses reveals a tendency for decreasing confinement with decreased amplitude.

Cross correlation measurements show the high-frequency pump-wave amplitude modulations and low-frequency density perturbations are strongly related, but quantitative estimates are at present limited to the longest system time scale τ_3 [Fig. 1(b)]. Figure 4 shows outputs from a signal averager fed by the ion biased radial probe. The averaging for Fig. 4(a) and 4(b) is intiated by large-amplitude burst detected on axis, the outputs being recorded at $r = 0$ and 2.5 mm, respectively. The obvious feature is a periodic density

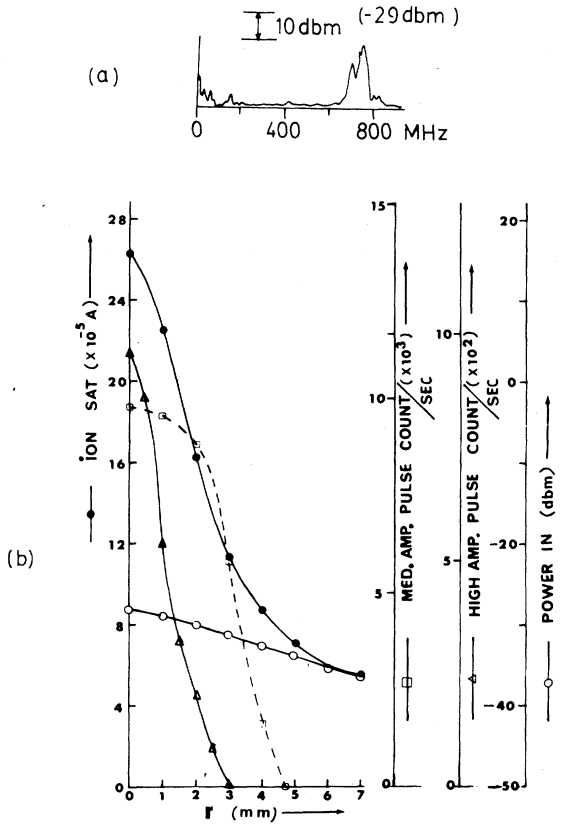

FIG. 3. (a) Frequency spectrum of electron cyclotron instability. f_{ce} = 550 MHz; f_{pe} = 600 MHz; beam energy = 250 eV; beam current = 5 mA. (b) Comparison of radial distribution of large- ($\geq$ 32 mV peak to peak) and medium- ($\geq$ 25 mV peak to peak) amplitude pulses with average power of the instability and density profile. Parameters as in (a).

oscillation arising from a beam-edge ion cyclotron harmonic (ICH) instability, but superimposed density depletions (arrowed) are also seen. In Fig. 4(a), the depletion is concurrent with the wave burst trigger, whereas in Fig. 4(b) ($r = 2.5$ mm) it is delayed, implying passage of a density perturbation radiating from the axis following the occurrence of the filamentary structures which collectively form a "τ_3" burst. The radial velocity of this depletion $V \sim 10^4$ cm/sec is much less than the ion thermal speed ($\sim 2 \times 10^5$ cm/sec) and corresponds roughly to the perpendicular group velocity of a large-wave-number ICH wave.

That such density depletions are not (within the system sensitivity) detected when lower-amplitude bursts trigger the system can be seen from Fig. 4(c), also recorded at $r = 0$.

We note that though the "τ_3" bursts and the

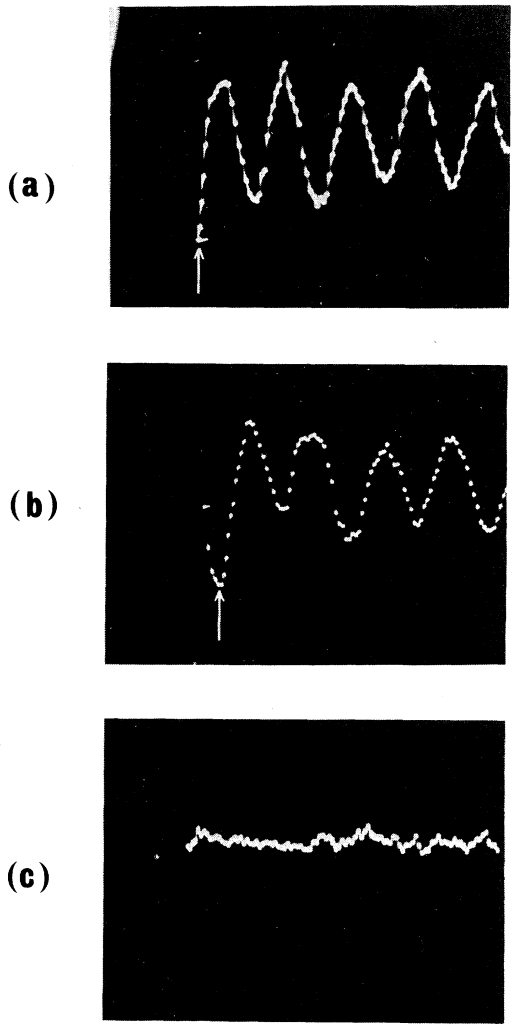

FIG. 4. Ion saturation current fluctuations associated with large-amplitude pulses (≥ 32 mV peak to peak) at (a) $r = 0$ mm; (b) $r = 2.5$ mm. (c) Ion saturation current fluctuations at $r = 0$ mm associated with intermediate-amplitude pulses (≥ 20 mV peak to peak). The horizontal scale is 10 μsec/mm. Arrows indicate superimposed density depletions.

beam-edge ICH wave have similar periodicities, and exhibit some coupling [see Figs. 4(a) and 4(b)] they are distinct phenomena, as evidenced by the form of their density perturbations, which for example show $m = 0$ and $m = 1$ azimuthal symmetries, respectively.

The density perturbation ratio $\Delta n/n$ associated with the strong bursts has an experimental lower limit of (2–3)%. Measurements of the burst amplitude are less certain because the probe efficiency η is not well known. From earlier linear wave propagation and beam trapping experiments[12] we estimate $\eta \sim -30$ to -40 dB giving a lower limit to the burst radial wave field of a few tens of volts per centimeter. Thus the approximate equality $\Delta n/n = E^2/8\pi nT$ is comfortably satisfied, though this static balance condition between plasma pressure and ponderomotive force is unlikely to apply strictly in such dynamic circumstances.

The axial scale length $L_\parallel$ of these collapsed structures is of great interest, but results from multiprobe spatial correlation measurements are at present irritatingly ambiguous. For waves of the upper hybrid branch, we can set an upper limit $\langle L_\parallel \rangle \sim 2$ cm though there is some evidence that this significantly overestimates $L_\parallel$ for the relatively infrequent large bursts.

The collapse time is inferred from real-time records such as Fig. 1(a) where cusped potential structuring evolves on time scales $\lesssim 1$ μsec ($\sim 1/f_{pi}, f_{lh}$), though one notes that the largest spikes, which exhibit the most dramatic radial collapse, occur quasirepetitively on ion cyclotron time scales.

The evolution of large amplitude into collapsed cigarlike structures ($L_\perp < L_\parallel$) may not be completely unexpected given the existence of transverse intensity gradients in the linear regime. The longer time scales τ_2, τ_3 associated with evolution and recurrence of these phenomena strongly imply nonlinear coupling to (and decoupling from) near-normal ion modes of the plasma, but the shortest times, $\tau_1 \sim 1/f_{pi}$, indicate that electron nonlinearities may be important. On the longest time scale the observations may fit loosely into a class of predicted solitary field aligned structures[8-10] and we note in particular that Dysthe *et al.*[10] predict cigarlike solutions (for the upper-hybrid branch) reminiscent of those reported here.

The results indicate that some elaboration of the one-dimensional aspects of collapse phenomena, in which the bulk of work in the area of strong turbulence has been concentrated, may be warranted.

In this work we have benefited from stimulating conversation with M. I. Woodhill, C. M. Lashmore-Davies, M. J. Giles, and V. I. Karpman. Support from the United Kingdom Atomic Energy Authority Culhum Laboratory and, for one of us (V. K. J.), the Indian Ministry of Education, is gratefully acknowledged.

[1]H. Ikezi, K. Nishikawa, and K. Mima, J. Phys. Soc. Jpn. 37, 766 (1974).

[2]A. Y. Wong and B. H. Quon, Phys. Rev. Lett. 34,

1499 (1975).
[3]H. Ikezi, R. P. H. Chang, and R. A. Stern, Phys. Rev. Lett. 36, 1047 (1976).
[4]S. V. Antipov, M. V. Nezlin, E. M. Snezhkin, and A. S. Trubnikov, Zh. Eksp. Teor. Fiz. 47, 965 (1978) [Sov. Phys. JETP 47, 506 (1978)].
[5]S. V. Antipov, M. V. Nezlin, E. N. Snezhkin, and A. S. Trubnikov, Zh. Eksp. Teor. Fiz. 49, 1571 (1979) [Sov. Phys. JETP 49, 797 (1979)].
[6]V. E. Zakharov, Zh. Eksp. Teor. Fiz. 62, 1745 (1972) [Sov. Phys. JETP 62, 908 (1972)].
[7]L. M. Degtyarev, V. E. Zakharov, and L. I. Rudakov, Zh. Eksp. Teor. Fiz. 41, 115 (1975) [Sov. Phys. JETP 41, 57 (1975)].
[8]M. Porkolab and M. V. Goldman, Phys. Fluids 19, 872 (1976).
[9]M. Y. Yu and P. K. Shukla, Plasma Phys. 19, 889 (1977).
[10]K. B. Dysthe, E. Mjølhus, H. L. Pecseli, and L. Stenflo, Plasma Phys. 20, 1087 (1978).
[11]N. S. Buchelnikova and E. P. Matochkin, Plasma Phys. 23, 35 (1981), and references therein.
[12]C. A. Nyack and P. J. Christiansen, Phys. Fluids 17, 2025 (1974).

Long-Wavelength Magnetohydrodynamic Stability of the Field-Reversed Theta Pinch

D. C. Barnes[a]
Los Alamos National Laboratory, Los Alamos, New Mexico 87545

and

D. V. Anderson
National Magnetic Fusion Energy Computer Center, Lawrence Livermore National Laboratory, Livermore, California 94550

(Received 23 January 1981)

The ideal magnetohydrodynamic equilibrium and stability of a field-reversed theta pinch is investigated. Elongated, scalar pressure equilibria with no toroidal field are generated by a two-dimensional equilibrium code. Their stability is investigated in three-dimensional, nonlinear magnetohydrodynamic simulations. Experimental equilibria and stability properties are reproduced.

PACS numbers: 52.55.Ez, 52.30.+r

In the field-reversed theta pinch (FRTP) experiments FRX-*A* and FRX-*B*,[1] as in other FRTP experiments,[2] a compact toroidal plasma is produced. During a confinement time of tens of Alfvén transit times, no magnetohydrodynamic (MHD) instabilities are observed. Later a rotating, $n=2$ mode disrupts the plasma only after it rotates rigidly above a critical velocity. If ideal MHD theory applies, catastrophic MHD activity should destroy the stationary equilibrium. Earlier theories showed the large-scale, rapidly growing MHD instabilities of a large-aspect, toroidal Z pinch.[3,4] Increasing the elongation decreases the growth rate only moderately and does not explain the observed stable period. Effects due to small aspect ratio, diffuse profile, or some other physics such as finite Larmor radius (FLR) may suppress MHD instabilities.

Our fully three-dimensional (3D) calculations include all geometric effects, but resolve only large-scale modes. FLR and other physics which strongly affect shorter-wavelength modes are ignored. However, in a very crude sense, the cutoff in wave number associated with finite grid size might represent such effects in a real plasma (the grid spacings are about a gyrodiameter).

Only a poloidal field is considered. Assuming a pressure $P=P(\psi)$, $\psi=rA_\theta$, and denoting $\partial/\partial\psi$ by a prime the equilibrium equation is

$$\frac{\partial^2\psi}{\partial z^2}+\frac{\partial^2\psi}{\partial r^2}-\frac{1}{r}\frac{\partial\psi}{\partial r}=-r^2P'. \tag{1}$$

Equation (1) is solved on a two-dimensional (2D), r-z mesh with use of the CYLEQ[5] code. With a $P(\psi)$ containing both hollow and peaked current parts

$$P(\psi)=(1-H)P_1\left(\frac{\psi_s-\psi}{\psi_s-\psi_v}\right)^m + \frac{HP_1}{2}\left\{1+\cos\left[\pi\left(\frac{\psi-\psi_v}{\psi_s-\psi_v}\right)^m\right]\right\}, \tag{2}$$

equilibria consistent with the measured plasma parameters in FRX-*A* are obtained. Here ψ_s and ψ_v give ψ at the plasma surface and vortex (zero point), respectively. H is the fraction of the hollowed current desired (usually $H=\frac{1}{2}$). P_1 is the pressure maximum.

(a)

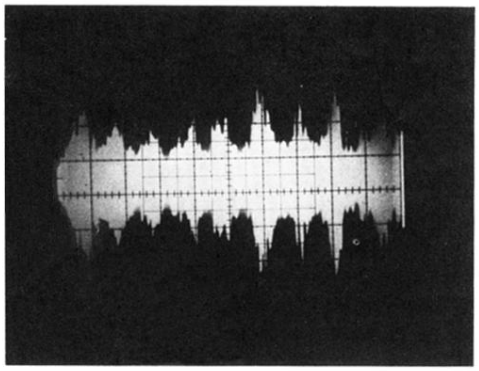

(b)

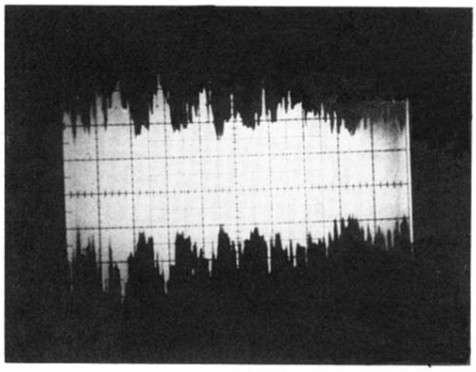

FIG. 1. Real-time observations of wave burst structure. (a) Horizontal scale, 2 μsec/div; vertical scale, 10 mV/div. (b) Horizontal scale, 200 μsec/div; vertical scale, 10 mV/div.

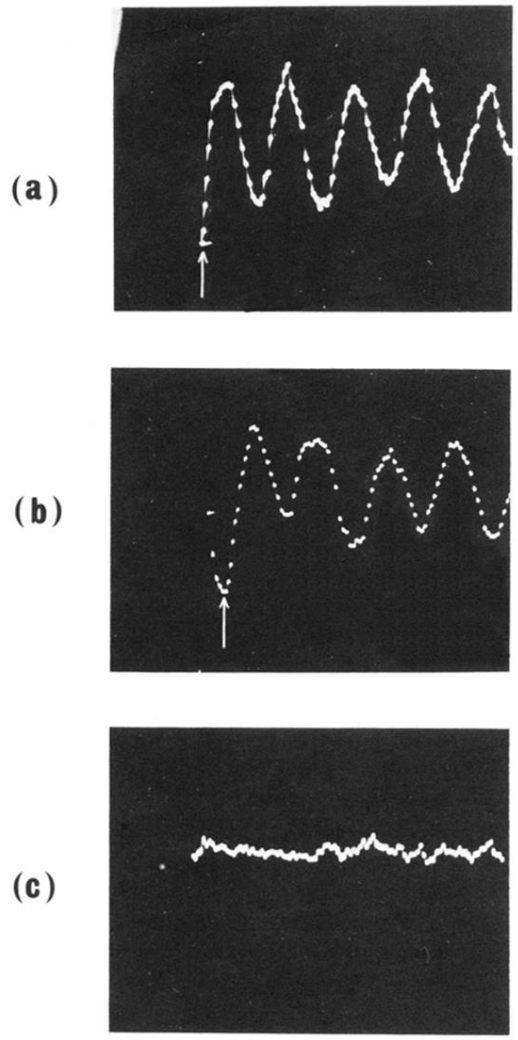

FIG. 4. Ion saturation current fluctuations associated with large-amplitude pulses ($\geq$ 32 mV peak to peak) at (a) r = 0 mm; (b) r = 2.5 mm. (c) Ion saturation current fluctuations at r = 0 mm associated with intermediate-amplitude pulses ($\geq$ 20 mV peak to peak). The horizontal scale is 10 μsec/mm. Arrows indicate superimposed density depletions.